

# Structural evolutions from polycarbosilane to SiC ceramic

G. D. SORARU\*, FLORENCE BABONNEAU†, J. D. MACKENZIE

*Department of Materials Science and Engineering, University of California, Los Angeles, California 90024, USA*

The pyrolysis process of a polycarbosilane into a microcrystalline silicon carbide ceramic has been followed up to 1700°C mainly by means of solid state  $^{29}\text{Si}$  and  $^{13}\text{C}$  nuclear magnetic resonance, transmission electron microscopy and X-ray diffraction analysis. A structural model has been proposed for the amorphous silicon carbide phase that is formed during the pyrolysis process. The ceramic obtained at high temperature is formed by a mixture of  $\beta$ -SiC and  $\alpha$ -SiC; however, some difficulties in the identification of the crystalline phases have been pointed out.

## 1. Introduction

Recently, it has been shown that non-oxide ceramics such as carbides and nitrides can be obtained by firing suitable metal-organic polymer precursors in controlled atmospheres [1]. A common feature of the polymer route to carbides or nitrides is the formation of intermediates which are amorphous solids. These are formed after the removal of the organic components and before crystallization [2]. We have already pointed out the importance of regarding these amorphous covalent ceramics (ACC) as an entirely new family of disordered solids whose structure and properties are worthy of independent study [3, 4].

Among the various systems already synthesized, SiC obtained from polycarbosilane is certainly the most widely studied [5-7]. Commercially available Nicalon SiC fibres are obtained from polycarbosilane following the process first developed by Yajima *et al.* [8]. The feasibility of this method in producing fibres or coatings is not restricted to this material. It is mainly due to the polymeric nature of the ceramic precursors, and it accounts for the many research efforts that are currently being conducted. Despite the increasing number of studies on SiC fibres obtained by the Yajima process, the structural conversion from the starting polycarbosilane to the resulting ceramic material is not well understood. In this paper the pyrolysis mechanism of polycarbosilane, the structure of the intermediate ACC phase and its conversion into the microcrystalline silicon carbide ceramics, will be discussed mainly based on  $^{29}\text{Si}$  and  $^{13}\text{C}$  magic-angle spinning nuclear magnetic resonance (MAS-NMR), electron spin resonance (ESR), X-ray diffraction (XRD) and transmission electron microscopy/selected area electron diffraction (TEM/SAED) experiments.

## 2. Experimental procedure

Commercially available polycarbosilane (PC, Dow Corning X9-6348) with a molecular weight of 1400,

was used in this study. All the firing treatments were performed in flowing argon with a heating rate of  $2^\circ\text{C min}^{-1}$  up to the complete removal of the organic components at around 840°C. The resulting inorganic solid, that is amorphous according to XRD and TEM/SAED experiments, can be considered as the ACC phase precursor for SiC microcrystalline ceramics. In order to study the subsequent densification and crystallization process, the ACC phase was fired at different temperatures up to 1700°C at  $10^\circ\text{C min}^{-1}$ . The amounts of silicon, carbon and hydrogen were analysed for selected samples. Oxygen content was not analysed. Thermogravimetric analysis was performed in flowing argon using a Perkin Elmer equipment.  $^{29}\text{Si}$ ,  $^{13}\text{C}$  and  $^1\text{H}$  liquid NMR spectra were recorded on a AM 360 Bruker spectrometer at 71.5, 90.5 and 360 MHz, respectively. The polymer was dissolved in  $\text{CDCl}_3$ . For  $^{29}\text{Si}$  NMR experiments, a pulsewidth of  $10\ \mu\text{sec}$  was applied with a relaxation delay of 6 sec.  $^1\text{H}$  and  $^{13}\text{C}$  NMR spectra were recorded with pulsewidths of  $2\ \mu\text{sec}$  for  $^1\text{H}$  and  $5\ \mu\text{sec}$  for  $^{13}\text{C}$ , and delays between pulses of 1 sec for  $^1\text{H}$  and 2 sec for  $^{13}\text{C}$ . Solid-state  $^{29}\text{Si}$  and  $^{13}\text{C}$  NMR spectra were obtained on a MSL 300 Bruker spectrometer at 59.6 and 75.5 MHz. A pulsewidth of  $2.5\ \mu\text{sec}$  and a delay between pulses of 60 sec were used for the  $^{29}\text{Si}$  MAS-NMR spectra. A contact time of 2 msec was applied for the cross-polarization experiments.  $^{13}\text{C}$  CP MAS-NMR spectra were recorded with a contact time of 3 msec. Tetramethylsilane (TMS) was used as a reference for all the NMR data. ESR experiments were carried out on a Varian E09 spectrometer. A Bruker gaussmeter was used to measure the magnetic field with diphenylpicrylhydrazyl (DPPH) as a standard. The number of spins was estimated by comparison with copper sulphate as reference. XRD patterns were recorded on a Philips diffractometer using a  $\text{CuK}\alpha$  radiation with a nickel filter. For TEM observations the samples were ground to very fine

\* Permanent address: Dipartimento di Ingegneria, Università di Trento, 38050 Mesiano, Trento, Italia.

† Permanent address: Chimie de la Matière Condensée, Université Paris 6, Tour 54, 4 place Jussieu, 75005 Paris, France.

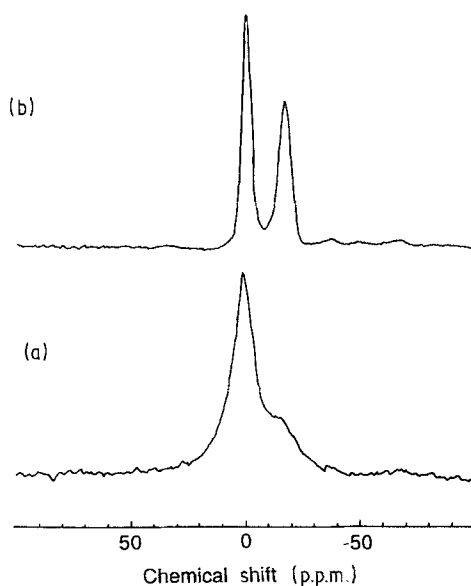


Figure 1 (a)  $^{29}\text{Si}$  MAS-NMR and (b)  $^{29}\text{Si}$  CP MAS-NMR spectra of polycarbosilane.

powders which were then dispersed on to a TEM copper grid using an eye dropper. TEM/SAED investigations were performed using a Jeol STEM 100 CX equipment. Density measurements were performed on fine powders by immersion in  $\text{CCl}_4$  following the Archimedes method. BET measurements were done with a Flow Sorb II 2300 Micromeritics equipment.

### 3. Results

#### 3.1. Characterization of the polymer precursor

The chemical analysis of PC, reported in Table I, shows a Si:C:H ratio of 1:2.2:5.  $^{29}\text{Si}$  MAS-NMR and  $^{29}\text{Si}$  CP MAS-NMR spectra have been recorded on this starting material (Fig. 1). The two spectra reveal the same features, with an enhancement of the resolution for the cross-polarized spectrum. The spectra show two different silicon units, already reported in the literature [7]. The peak at  $-0.8$  p.p.m. is due to silicon atoms bonded to four carbon atoms ( $\text{SiC}_4$ ) as type I units and the second peak at  $-17.6$  p.p.m. is due to type II units in which the silicon atoms are surrounded by three carbon atoms and one hydrogen atom ( $\text{SiC}_3\text{H}$ ). No distinct peaks appear around  $-35$  p.p.m.: Si-Si bonds, if they exist, are thus not abundant in this starting PC [7]. These two types of units are shown below.

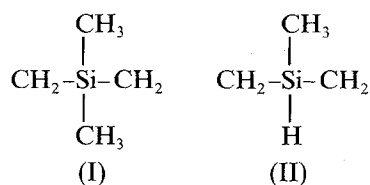


TABLE I Atomic ratio Si:C:H in the precursor and in some fired samples

Sample	Si	C	H
PC	1	2.2	5
PC840	1	1.6	0.65
PC1200	1	1.44	0.10
PC1500	1	1.43	0.07

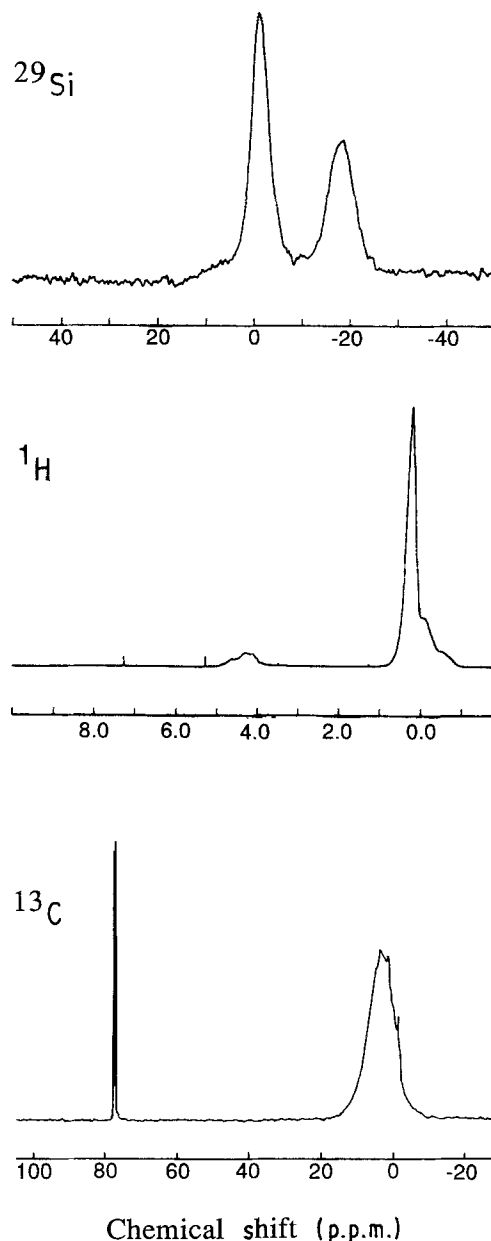


Figure 2  $^{29}\text{Si}$ ,  $^1\text{H}$  and  $^{13}\text{C}$  NMR spectra of polycarbosilane dissolved in  $\text{CDCl}_3$ .

PC was dissolved in  $\text{CDCl}_3$ .  $^{29}\text{Si}$ ,  $^1\text{H}$  and  $^{13}\text{C}$  NMR spectra were recorded in solution (Fig. 2). The  $^{29}\text{Si}$  NMR spectrum is quite similar to the CP MAS-NMR spectrum on the powder. The ratio between the two kinds of units (I and II) appears to be 1:0.8. The  $^1\text{H}$  NMR spectrum of PC shows two regions for the resonance, from 4 to 5 p.p.m. due to Si-H bonds and around 0 p.p.m. due to C-H bonds. The integration of the peaks gives a value of 11 for the C-H/Si-H ratio. In the Si-H region, several peaks are present at 4.1, 4.3 and 4.6 p.p.m. due to different Si-H sites. The C-H region shows a main peak at 0.17 p.p.m., due to  $\text{CH}_3$  groups, and two shoulders with lower chemical shift values, at 0 and 0.5 p.p.m. assigned, respectively, to  $\text{CH}_2$  and  $\text{CH}$  groups. The  $^{13}\text{C}\{-^1\text{H}\}$  spectrum of the solution shows a broad peak centred on 3 p.p.m. corresponding to the aliphatic carbon atoms present in PC in  $\text{CH}_3$ ,  $\text{CH}_2$  and  $\text{CH}$  units. Some sharp peaks are superimposed, certainly due to some quite mobile units inside the polymer.

All the NMR spectra indeed have broad peaks, and

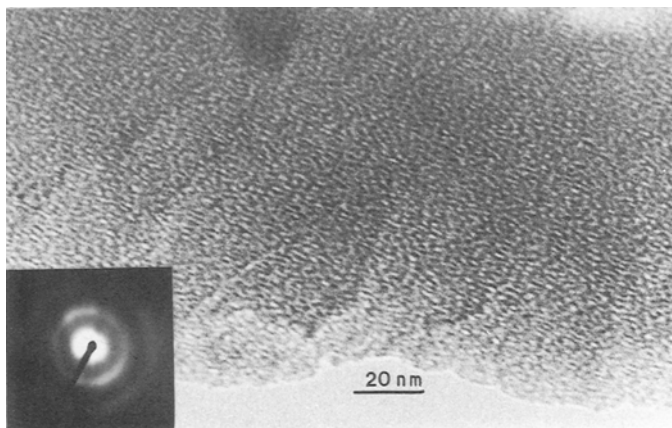
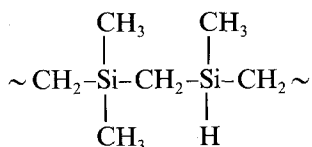


Figure 3 TEM bright-field micrograph with SAED patterns of polycarbosilane pyrolysed at 840°C.

no resolution was obtained especially for  $^1\text{H}$  and  $^{13}\text{C}$  NMR experiments. This seems to indicate that a large distribution of units is present in this polycarbosilane. The structure of polycarbosilane that emerges from these results is more complicated than a simple linear chain of type I and II units with a 1:1 ratio such as



In this case the chemical analysis should be  $\text{Si}:\text{C}:\text{H} = 1:2.5:7$ . The low carbon and hydrogen contents in the studied PC and the presence of CH units in the  $^1\text{H}$  NMR spectrum suggest that some cross-linking has already occurred between the chains. This has already been suggested by Okamura *et al.* [9].

### 3.2. Characterization of the pyrolysis process

#### 3.2.1. From the precursor polymer to the ACC phase

The low molecular weight components of the polycarbosilane have been previously removed by melting the polymer in flowing nitrogen gas. Thermogravimetric analysis (TGA) performed on this material (PCD) showed that the weight losses end at around 800°C. At this temperature the precursor polymer has been converted into an inorganic solid that appears to be amorphous by XRD and TEM/SAED investigations (Fig. 3).

According to TGA experiments, the pyrolysis process leading to the formation of the amorphous silicon carbide phase, consists of two stages: from 300 to 500°C with a weight loss of 13% and from 500 to 800°C with a further weight loss of 12%. The PCD was heated at  $2^\circ\text{C min}^{-1}$  in argon up to 500°C (PC500), 700°C (PC700) and 840°C (PC840). The chemical analysis of PC840 appeared to be  $\text{Si}:\text{C}:\text{H} = 1:1.6:0.65$  (Table I). Excess carbon

was thus present in this amorphous silicon carbide phase.

The  $^{29}\text{Si}$  MAS-NMR and  $^{13}\text{C}$  CP MAS-NMR spectra recorded on these samples are shown in Fig. 4 as well as the spectra of the precursor as reference. The  $^{29}\text{Si}$  MAS-NMR spectrum of PC shows the two peaks assigned to  $\text{SiC}_4$  and  $\text{SiC}_3\text{H}$  units. In the sample fired at 500°C, the peak at  $-16$  p.p.m. assigned to the  $\text{SiC}_3\text{H}$  units has disappeared. The major peak at 0 p.p.m. due to  $\text{SiC}_4$  units appears almost unchanged with only a slight shift of the position of the maximum and a small increase of the linewidth (Table II). By increasing the firing temperature over 500°C and up to 840°C this trend is maintained: the peak related to the  $\text{SiC}_4$  units is continuously moving toward lower values of chemical shift typical of the crystalline silicon carbide phase while its linewidth is increasing up to 700°C. The evolution of the  $^{29}\text{Si}$  MAS-NMR spectra has already been explained in detail in a previous study [3]. In the first stage of the pyrolysis process, up to 500°C, a possible reaction is the consumption of Si-H groups and the formation of bridging Si-C bonds between the polycarbosilane chains. Above this temperature the shift of the peak due to  $\text{SiC}_4$  units reflects an increase of the connectivity

TABLE II  $^{29}\text{Si}$  MAS-NMR data for the precursor and the fired samples

Sample	Chemical shift (p.p.m.)	Linewidth (p.p.m.)
PC	0 16	10
PC500	-4.5	12.5
PC700	-6.3	34
PC840	-8.0	34

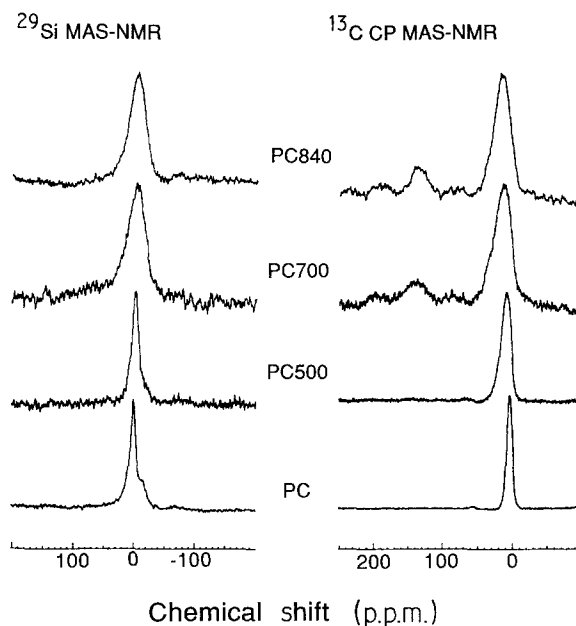


Figure 4 Evolution with the firing temperature of  $^{29}\text{Si}$  MAS-NMR and  $^{13}\text{C}$  CP MAS-NMR spectra of polycarbosilane.

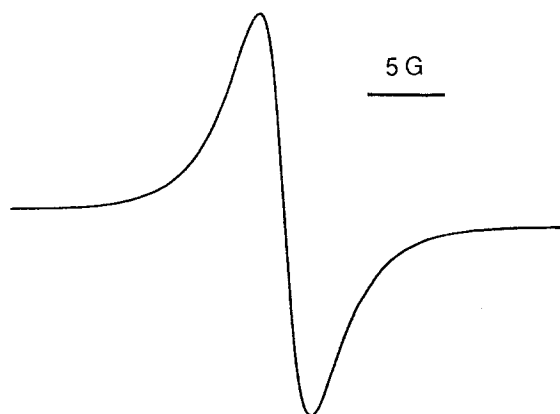


Figure 5 ESR spectrum recorded at room temperature on PC840.

of the network by the formation of Si–C–Si bonds. At the same time the evolution of the linewidth is correlated to an increase of the disorder of the local environment around the silicon atoms. During the pyrolysis process, condensation reactions lead to the consumption of CH<sub>3</sub> and CH<sub>2</sub> groups and to the formation of CH or C units with the evolution of H<sub>2</sub> or CH<sub>4</sub> [7]. These reactions obviously increase the number of different SiC<sub>4</sub> units that can exist in the material and may account for the observed increase of the peak linewidth already mentioned. <sup>29</sup>Si MAS-NMR study of the fired samples shows no other peaks than those assigned to SiC<sub>4</sub> units. No Si–Si nor Si–O bonds seem to be formed during the pyrolysis process.

Information about the evolution of the local environment of the carbon sites during the pyrolysis process can be obtained from the <sup>13</sup>C CP MAS-NMR spectra in Fig. 4. The spectrum of PC shows one peak at 4.2 p.p.m. and a small absorption near 55 p.p.m. that has been identified as a spinning side band. By increasing the firing temperature the main peak shifts toward higher values of chemical shift with a corresponding increase of its linewidth. The resonance present at 4.2 p.p.m. in the spectrum of PC is due to the contribution of all the carbon groups present in the starting polymer, namely CH<sub>3</sub>, CH<sub>2</sub> and CH. It is well known that the chemical shifts of CH<sub>n</sub> units increase when the *n* value is decreased. Then, according to these data, the shift of the peak with the firing temperature reflects a consumption of the more hydrogenated species due to the occurrence of the condensation reactions during the pyrolysis process. The increase in the linewidth has to be related with the same evolution in the <sup>29</sup>Si MAS-NMR spectra. It reveals an increase in the disorder of the local environment of the aliphatic carbon atoms during the pyrolysis process. Moreover, an interesting feature appears at above 700°C: new peaks are present in the 100 to 200 p.p.m. range. These peaks become more intense at 840°C. The broad peak centred around 135 p.p.m., can be assigned to the presence of aromatic carbon atoms, and could be related to the formation of C=C bonds. It has already been suggested that such bonds could be present in the intermediate amorphous phase but no experimental evidence was given. They should be precursor bonds for graphitic carbon that is formed around 1200°C according to Raman data [9].

ESR was performed on the sample fired at 840°C

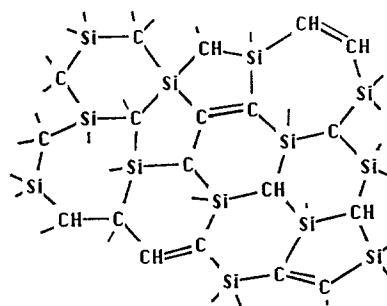


Figure 6 Proposed structure of the amorphous silicon carbide phase obtained from polycarbosilane.

(Fig. 5). The spectrum exhibits a single isotropic signal centred at  $g = 2.0030$ , with a linewidth of 3.9 G. This value corresponds to carbon dangling bonds [10]. The integration of the signal gave the number of defects to be  $2.5 \times 10^{19} \text{ cm}^{-3}$ , considering a density of  $2.2 \text{ g cm}^{-3}$  for this sample. This value is in agreement with the number of defects found in amorphous SiC<sub>1.5</sub> samples prepared from chemical vapour deposition [10].

### 3.2.2. Characterization of the ACC phase

The proposed structure of the amorphous silicon carbide phase obtained at 840°C is illustrated in Fig. 6. It is based mainly on the <sup>29</sup>Si MAS-NMR and <sup>13</sup>C CP MAS-NMR results although the broadness of the NMR peaks in these samples made it difficult to obtain precise structural data. These amorphous phases show a wide distribution of silicon and carbon atoms types. However, some relevant features can be pointed out. (a) The silicon carbide phase is not stoichiometric, but an excess of carbon is present (C/Si = 1.6). (b) All the silicon atoms seem to be bonded to four carbon atoms and Si–Si or Si–H bonds, if they are present should be minimal. (c) Some C=C bonds are present as clearly shown by the <sup>13</sup>C CP MAS-NMR experiments. (d) The residual hydrogen content (H/Si = 0.65) should be mainly present in the structure as CH groups as suggested by the chemical shift of the main peak in the <sup>13</sup>C CP MAS-NMR spectra. (e) The condensation reactions occurring during the pyrolysis process can lead to the formation of six-member rings like those present in crystalline SiC, but the formation of distorted five- or seven-atom rings cannot be ruled out and should lead to the presence of C–C bonds. (f) The presence of paramagnetic defects has been shown by ESR experiments and these defects were assigned to carbon dangling bonds.

A density of  $2.21 \text{ g cm}^{-3}$  has been measured on a sample of fine powders of this phase. This value is lower than the density of  $\beta$ -SiC ( $3.21 \text{ g cm}^{-3}$ ). A theoretical density ( $2.70 \text{ g cm}^{-3}$ ) can be estimated from the chemical analysis of PC840 (Table I) by using the rule of mixtures and assuming that all the silicon atoms are engaged in forming amorphous SiC (density  $3.0 \text{ g cm}^{-3}$ ) [11] while the remaining carbon is present as graphite (density  $2.2 \text{ g cm}^{-3}$ ). The low value of the density of the amorphous phase cannot be ascribed to the presence of porosity in the material. SEM investigations (Cambridge Sterescan) have shown only few

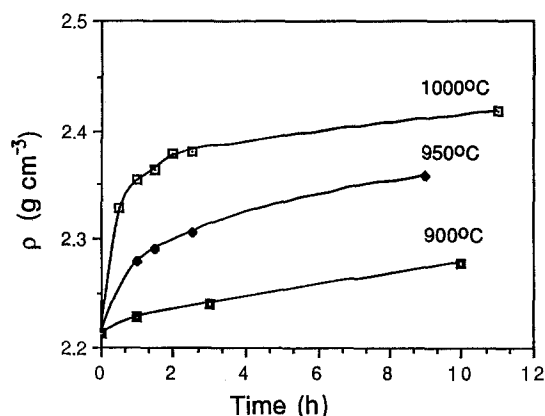


Figure 7 Evolution of the density,  $\rho$ , of the ACC phase with the firing time.

isolated pores for the ACC phase while TEM studies (Fig. 3) have shown no porosity at a sub-microscopic level. This evidence is also supported by BET analysis that gave a value of surface area lower than  $1 \text{ m}^2 \text{ g}^{-1}$  for the same sample. Therefore, a quite open structure, with a large amount of free volume must be invoked to account for the low value of density of the amorphous ceramics. With the aim of following the evolution of the density of PC840 as a function of the firing time, isothermal treatments in an argon atmosphere at 900, 950 and  $1000^\circ \text{C}$  were performed and the results reported in Fig. 7. An activation energy of  $82 \text{ kcal mol}^{-1}$  was obtained from the initial slope of the densification curves (Fig. 8). Assuming a negligible value of porosity in PC840, the observed increase of density during the firing treatment must be primarily ascribed to a reduction of its free volume. Two main processes may account for this effect. (i) The progress of the condensation reactions between residual CH groups in the structure with the elimination of  $\text{H}_2$  and  $\text{CH}_4$  and the formation of new Si-C-Si bridges with a consequent increase of the cross-linking of the network. Actually, chemical analysis of the ACC phase fired at 950 and  $1000^\circ \text{C}$  for the longest times, showed a decrease of the hydrogen down to  $\text{H/Si} = 0.2$  compared to the initial value of  $\text{H/Si} = 0.65$ ; (ii) a rearrangement of the open amorphous covalent structure toward more compact configurations with no change in chemical composition. For both of these mechanisms, a key step should be the cleavage of chemical bonds, either C-H ( $99 \text{ kcal mol}^{-1}$ ) in the first case or Si-C ( $76 \text{ kcal mol}^{-1}$ ) and C-C ( $82 \text{ kcal mol}^{-1}$ ) [12] in

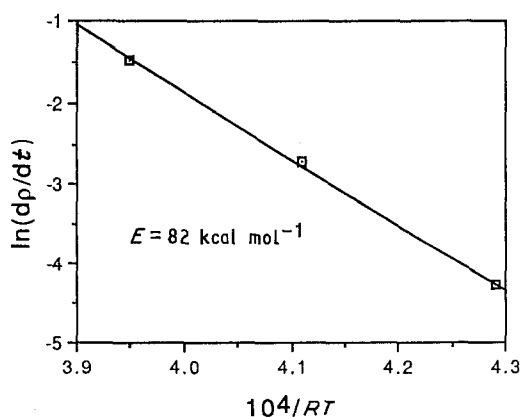


Figure 8 Arrhenius plot for the initial densification rate.

the latter one. The obtained value of activation energy suggests that, at least in the initial stages, the densification process occurs via the cleavage of chemical bonds present in the material. On the ground of  $^{29}\text{Si}$  MAS-NMR experiments, it has already been reported in a previous study [3] that, during the isothermal treatments, the rearrangement of the structure leads to an ordering of the local environment of the silicon atoms. Moreover, at the highest temperature ( $1000^\circ \text{C}$ ), XRD and TEM/SAED investigations showed a concomitant reorganization of the network also in the medium range with the formation of SiC microcrystals [3].

### 3.2.3. From the ACC phase to microcrystalline SiC

The amorphous silicon carbide phase can be converted into a microcrystalline ceramic by firing it at high temperatures. In order to follow such transformation, the PC840 was heated at  $10^\circ \text{C min}^{-1}$  in argon flow at  $1000^\circ \text{C}$  (PC1000),  $1200^\circ \text{C}$  (PC1200),  $1500^\circ \text{C}$  (PC1500) and  $1700^\circ \text{C}$  (PC1700). XRD and  $^{29}\text{Si}$  MAS-NMR spectra recorded on these samples are shown in Figs 9a and b, respectively, together with the spectra obtained on a commercial  $\beta$ -SiC as reference.

In the XRD patterns (Fig. 9a), broad peaks, corresponding to crystalline SiC phase, start to appear at  $1000^\circ \text{C}$  and sharpen by increasing the firing temperature. The corresponding crystallite sizes, evaluated from the diffraction results by using a peak broadening procedure, are reported in Table III. The microstructure of the sample heated at  $1500^\circ \text{C}$ , as revealed by TEM investigations, is shown in Fig. 10. Although a detailed analysis of the crystal sizes from TEM micrographs was not performed, the mean crystal size seems to be slightly higher compared to XRD results. This could be due to the fact that the crystallites have a range of size distribution in the sample and the largest particles are more readily observed. Fine porosity, as revealed by the white spots in the micrograph, seems to be present in this sample. This observation is in agreement with a recent study [13] that showed the formation of porosity in Nicalon fibres after annealing at  $1400^\circ \text{C}$  in argon atmospheres. BET analysis resulted in a value of surface area lower than  $1 \text{ m}^2 \text{ g}^{-1}$  indicating that closed porosity is present in these samples.

The position of the diffraction lines in the fired samples indicates that the microcrystalline phase is mainly  $\beta$ -SiC. In the XRD pattern of the sample heated up to  $1700^\circ \text{C}$  a small shoulder is seen at around  $2\theta = 34^\circ$ . It has been assigned to  $\alpha$ -SiC, suggesting that, at the highest temperatures the crystalline phase consists of a mixture of cubic  $\beta$ -SiC with traces of the hexagonal form.

TABLE III Sizes of the SiC microcrystals in the fired polycarbosilane calculated from the broadness of the main peak in the diffraction pattern

	Firing temperature ( $^\circ \text{C}$ )			
	1000	1200	1500	1700
Crystal size (nm)	1.5	2.5	8.0	16.0

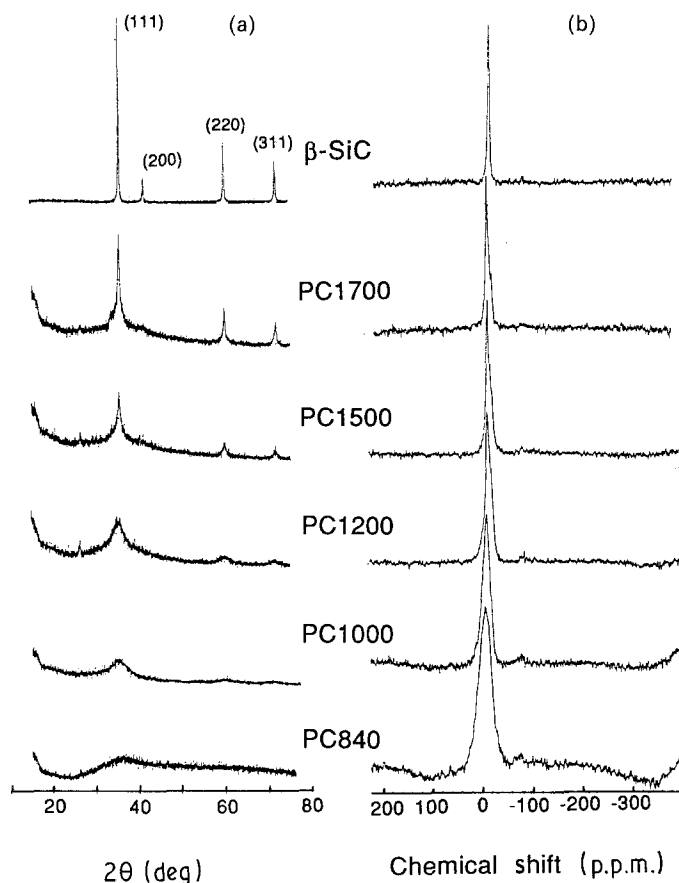


Figure 9 Evolution of (a) XRD patterns and (b)  $^{29}\text{Si}$  MAS-NMR spectra of ACC phase during the firing process ( $\beta$ -SiC sample provided by Superior Graphite).

In the X-ray patterns of the fired samples a small peak around  $2\theta = 26^\circ$  is clearly visible. Its intensity reaches the maximum value in the sample heated at  $1200^\circ\text{C}$  and decreases with further heating. It could be assigned either to the (101) reflection of  $\alpha$ -quartz or to the (002) line of carbon. In the literature, the disappearance of this peak after a treatment with HF has been reported [7]. This result has been assumed to be proof for the existence of crystalline silica in the fired ceramics. However, in the present study, the samples were heated in an inert atmosphere to avoid major oxygen contamination; moreover  $\text{SiO}_4$  units should give rise to a peak in the  $^{29}\text{Si}$  MAS-NMR spectra around  $-110$  p.p.m. Such a peak is completely absent in the spectra. Therefore it seems that the X-ray diffraction peak at  $2\theta = 26^\circ$  should be assigned to the presence of small clusters of graphite rather than crystallites of  $\alpha$ -quartz.

The evolution with the firing temperature of the  $^{29}\text{Si}$  MAS-NMR spectra is shown in Fig. 9b. The main peak corresponding to the  $\text{SiC}_4$  units is shifting down-field approaching the value corresponding to the crystalline form (Table IV). At the same time, its linewidth is decreasing suggesting an ordering of the local environment of the silicon atoms in the  $\text{SiC}_4$  units. At  $1500^\circ\text{C}$  some structures start to appear in this peak that become more evident at  $1700^\circ\text{C}$ . At this temperature, the MAS-NMR spectrum reveals three

distinct peaks at  $-16.2$ ,  $-20$  and  $-25$  p.p.m. Such a spectrum has already been published in the literature [14, 15]. In a first approximation, the main peak at  $-16.2$  p.p.m. can be assigned to  $\beta$ -SiC and the two minor peaks could be due to some  $\alpha$  phase. However, this assignment will be discussed later in the discussion.

#### 4. Discussion and conclusion

In the pyrolysis of PC, the removal of organic components occur via condensation reactions between  $\text{CH}_3$  and  $\text{CH}_2$  groups of the starting polymer. When this process is complete the polymer has been converted into an amorphous covalent ceramic (ACC) phase. The temperature at which the condensation reactions end and the ACC is formed can be obtained from a TGA experiment: it can be defined as the temperature at which the weight losses are complete and the curve approaches a constant weight value. However, this is

TABLE IV  $^{29}\text{Si}$  MAS-NMR data of the fired polycarbosilane

	PC840	PC1000	PC1200	PC1500	PC1700
Chemical shift (p.p.m.)	-8	-15	-16	-16.2	-16.2
				-20	-20
				-25	-25

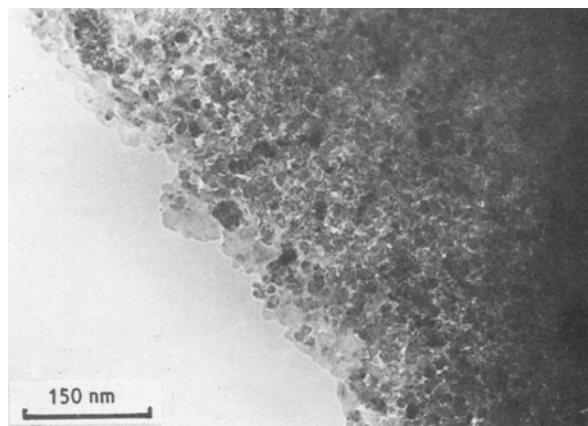


Figure 10 TEM bright-field micrograph of PC fired at  $1500^\circ\text{C}$ .

not an absolute threshold value: it is reasonable to think that the temperature of formation of the ACC phase is dependent upon the heating rate and the heating atmosphere. For example, by processing the PC in vacuum or by using a lower heating rate it should be possible to complete the pyrolysis process at lower temperature and thus it should be possible to get an amorphous inorganic solid at lower temperature. Moreover, the structure itself and the composition of the forming inorganic disordered phase can be affected by the same processing parameters i.e. temperature, heating rate and heating atmosphere.

In the present study, TGA experiments obtained using a heating rate of  $2^{\circ}\text{C min}^{-1}$  in flowing argon, showed that the weight losses end at around  $800^{\circ}\text{C}$ . Thus according to these results the PC has been converted into the ACC phase for the subsequent structural and crystallization studies by heating it with the same processing parameters at temperatures slightly higher than  $800^{\circ}\text{C}$ , namely  $840^{\circ}\text{C}$ .

A wide range of different types of defect seems to exist in this amorphous silicon carbide phase as shown in Fig. 6. NMR and ESR experiments showed the presence of C=C bonds and carbon dangling bonds respectively. The presence of distorted five- or seven-atom rings can be reasonably assumed [3]; excess carbon and residual hydrogen (C/Si = 1.6; H/Si = 0.65) have been evinced by chemical analysis. Chemical and structural modifications occur in this phase by increasing the temperature over  $840^{\circ}\text{C}$ . Residual hydrogen content and carbon excess are considerably reduced (Table I) at  $1200^{\circ}\text{C}$  (H/Si = 0.1; C/Si = 1.44) and are still decreasing at  $1500^{\circ}\text{C}$  (H/Si = 0.07; C/Si = 1.43) due mainly to the completion of condensation reactions. The other major modification occurring during the firing process of the ACC phase is its structural rearrangement that leads to the formation of a microcrystalline ceramic. This transformation starts, according to XRD and TEM/SAED experiments, at around  $1000^{\circ}\text{C}$ . It is known [16] that the crystallization mechanism of disordered covalent four-coordinated materials like amorphous silicon or germanium involves the rupture of the Si-Si or Ge-Ge bonds, respectively. In these cases the experimentally observed activation energies are close to the covalent bond energies for both silicon [17] and germanium [18]. In the present case, the crystallization mechanism of the amorphous silicon carbide phase should be more complicated because it occurs together with the mentioned chemical modification of the system. The crystallization of the ACC phase results in an increase of its density. Kinetic studies of the densification process in the early stages of crystallization, below  $1000^{\circ}\text{C}$ , gave an activation energy close to the energies of the Si-C and C-C bonds. However, it is not possible to regard this value as the activation energy for crystallization because the observed densification is due not only to crystallization but also to the concomitant completion of the condensation process.

At  $1200^{\circ}\text{C}$  crystallites of SiC with dimension of 2.5 nm are present in the material (Table III); bright-field TEM observations were still featureless like those obtained on PC840. However, the diffraction rings

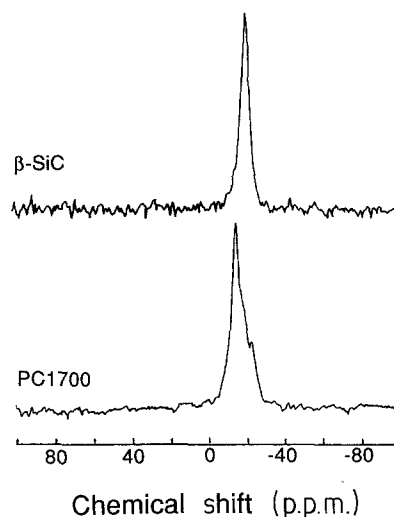


Figure 11 Comparison between the  $^{29}\text{Si}$  MAS-NMR spectra of the sample fired at  $1700^{\circ}\text{C}$  and a commercial  $\beta$ -SiC (Superior Graphite).

were quite narrow, confirming the microcrystalline nature of this sample. As suggested by X-ray diffraction patterns, clusters of graphite are present in the material. As already reported [19] they should be present at the edge of SiC microcrystals and could play an important role preventing or slowing the rate of crystal growth.

At  $1500$  and  $1700^{\circ}\text{C}$  the crystal size increase up to 8 and 16 nm, respectively (Table III). As reported in the literature [7] this process should be connected with an evolution of CO from the system. In the present case, however, if this reaction takes place, it, should be minimal concerning only the oxygen present in the system as impurities: indeed, in the firing process of PC care has been taken to avoid major oxygen contamination.

The density of the sample fired at  $1500^{\circ}\text{C}$  approaches the value of  $2.7\text{ g cm}^{-3}$ . The theoretical density, calculated as previously described from the chemical analysis and using in this case the density of  $\beta$ -SiC ( $3.2\text{ g cm}^{-3}$ ), is  $2.9\text{ g cm}^{-3}$ . The difference between the two values can be ascribed to a possible close porosity present in the sample as revealed by TEM observations. A value of 7% of porosity should account for the observed difference in the density values.

According to XRD analysis  $\beta$ -SiC seems to be the principal crystalline phase in the samples fired at the highest temperatures together with small amounts of the hexagonal form. The presence of  $\alpha$ -SiC in Nicalon fibres heated at temperatures higher than  $1400^{\circ}\text{C}$  has already been reported in the literature [13]. However, due to the broadness of the diffraction peaks, a definitive assignment seems difficult. Many different polytypes of the hexagonal phase are known, differing from each other only in the stacking sequence of the silicon and carbon layers [20].

$^{29}\text{Si}$  MAS-NMR has been successfully applied to distinguish between the different SiC polytypes [14, 21]. In Fig. 11 a comparison between the  $^{29}\text{Si}$  MAS-NMR spectrum of the sample fired at  $1700^{\circ}\text{C}$  and that recorded on commercial  $\beta$ -SiC is reported. The NMR spectrum of SiC from polycarbosilane shows three distinct peaks at  $-16.2$ ,  $-20$  and

TABLE V Chemical shifts of silicon carbide polytypes

Sample	Chemical shift (p.p.m.)	Reference
$\beta$ -SiC, 3C	-18.3	[21]
	-18.9	Present
$\alpha$ -SiC, 6H	-13.9	[21]
	-20.2	
	-24.5	
$\alpha$ -SiC, 15R	-14.9	[21]
	-20.8	
	-24.4	

-25 p.p.m. whereas the commercial one displays just one peak at -19 p.p.m. A detailed NMR study of silicon carbide polytypes has been published by Hartman *et al.* [21]. Among the large number of known polytypes, it seems that only four types of silicon environment exist, designated A, B, C and D by these authors. The cubic silicon carbide ( $\beta$  phase or 3C polytype) has only type A silicon sites, while the 6H or 15R polytypes exhibit three silicon sites A, B and C in relative intensities 1:1:1 and 1:2:2, respectively. The chemical shifts for these polytypes are reported in Table V. The type D site is more unusual: it is the only site present in the 2H polytype, but no NMR data seem available. The chemical shift has been predicted to be -31 p.p.m. [21]. The two resonances at -20 and -25 p.p.m. in the PC sample pyrolysed at 1700°C, can be assigned to the presence of type B and C silicon units of some  $\alpha$  phases. The third component due to type A units could lie under the major peak at -16.2 p.p.m. The assignment of this peak is more complicated, because the chemical shift does not correspond to the usually reported value for  $\beta$ -SiC. This value, around -16 p.p.m. has already been reported for powdered samples that were supposed to be  $\beta$ -SiC [14, 15], and also for  $\beta$ -SiC single crystals [22]. Inkrott *et al.* [15] found such peak in a plasma synthesized SiC sample. After annealing this material above 1600°C under inert atmosphere, the expected  $\beta$ -SiC peak at 18.3 p.p.m. appeared.  $\beta$ -SiC has only type A silicon units. However, the chemical shift is different from that of type A units in 6H or 15R polytypes (-13.9 and -14.9 p.p.m., respectively). Hartman *et al.* [21] assigned this difference to different Si-C bondlengths: in  $\beta$ -SiC, the silicon site has a full tetrahedral symmetry, while one long and three short Si-C distances are present in the 6H polytype. The anomalous peak around -16 p.p.m., can certainly be assigned to type A units. The shift compared to the 3C polytype could be due to a lower symmetry of the

silicon sites with slight differences in the Si-C bondlengths. This is only an assumption, and the identification of the crystalline phase formed during the pyrolysis process of PC seems worthy of further studies.

### Acknowledgements

Mike Jeckle and Richard Lysse are thanked for their respective contribution in the MAS-NMR and TEM/SAED investigations. NSF is also acknowledged for financial support of this study, Contract no. DMR 87 06379.

### References

1. K. J. WYNNE and R. W. RICE, *Ann. Rev. Mater. Sci.* **14** (1984) 297.
2. B. A. BENDER, R. W. RICE and J. R. SPANN, *J. Amer. Ceram. Soc.* **70** (1987) C58.
3. G. D. SORARU, F. BABONNEAU and J. D. MACKENZIE, *J. Non-Cryst. Solids* **106** (1988) 256.
4. G. D. SORARU, F. BABONNEAU and J. D. MACKENZIE, "Proceedings of the 7th International Symposium on Ceramics", 14 to 16 December 1988, Bologna, Italy, in press.
5. S. YAJIMA *et al.*, *J. Mater. Sci.* **13** (1978) 2569.
6. Y. HASEGAWA, M. HIMURA and S. YAJIMA, *ibid.* **15** (1980) 720.
7. Y. HASEGAWA and K. OKAMURA, *ibid.* **18** (1983) 3633.
8. S. YAJIMA, J. HAYASHI and M. OMORI, *Chem. Lett.* (1975) 931.
9. K. OKAMURA *et al.*, "Ultrastructure Processing of Advanced Ceramics", edited by J. D. Mackenzie and D. R. Ulrich (Wiley, New York, 1988) p. 501.
10. S. LIEDIKE *et al.*, *J. Non-Cryst. Solids* **97/98** (1987) 1083.
11. J. LIPOWITZ *et al.*, *Adv. Ceram. Mater.* **2** (1987) 121.
12. T. L. COTTRELL, "The Strength of Chemical Bonds" (Butterworths, London, 1958).
13. R. CHAIM, A. HEUER and R. T. CHEN, *J. Amer. Ceram. Soc.* **71** (1988) 960.
14. G. L. MARSHALL *et al.*, *Proc. Symp. Sci. Ceram.* **14** (1987) 347.
15. K. E. INKROTT, S. M. WHARRY and D. J. O'DONNELL, *Mater. Res. Soc. Symp. Proc.* **73** (1986) 155.
16. D. TURNBULL, *J. Non-Cryst. Solids* **75** (1985) 197.
17. L. CZEPREGI *et al.*, *J. Appl. Phys.* **49** (1978) 3906.
18. L. CZEPREGI *et al.*, *Solid State Commun.* **21** (1977) 1019.
19. J. AYACHE *et al.*, *J. Mater. Sci. Lett.* **7** (1988) 885.
20. V. HAASE *et al.*, "Gmelin Handbook of Inorganic Chemistry", (Springer, Berlin, Heidelberg, New York, 1984) Supplement Volume B2, Si-Silicon, "Properties of Crystalline Silicon Carbide".
21. J. S. HARTMAN *et al.*, *J. Amer. Chem. Soc.* **109** (1987) 6059.
22. J. R. GUTH and W. T. PETRUSKEY, *J. Phys. Chem.* **91** (1987) 5361.

Received 4 May  
and accepted 29 September 1989